Journal of Hazardous Materials 215–216 (2012) 75–82

Contents lists available at SciVerse ScienceDirect

Journal of Hazardous Materials

journal homepage: www.elsevier.com/locate/jhazmat

Kinetic and mechanistic study of microcystin-LR degradation by nitrous acid under ultraviolet irradiation

Qingwei Ma[a], Jing Ren[a], Honghui Huang[b], Shoubing Wang[a], Xiangrong Wang[a,*], Zhengqiu Fan[a,*]

[a] Department of Environmental Science & Engineering, Fudan University, Shanghai 200433, China
[b] Key Laboratory of Fisheries Ecology Environment, Ministry of Agriculture, Guangzhou 510300, China

ARTICLE INFO

Article history:
Received 4 November 2011
Received in revised form 5 February 2012
Accepted 13 February 2012
Available online 22 February 2012

Keywords:
Microcystin-LR
Ultraviolet
Nitrous acid
Kinetics
Degradation mechanism

ABSTRACT

Degradation of microcystin-LR (MC-LR) in the presence of nitrous acid (HNO_2) under irradiation of 365 nm ultraviolet (UV) was studied for the first time. The influence of initial conditions including pH value, $NaNO_2$ concentration, MC-LR concentration and UV intensity were studied. MC-LR was degraded in the presence of HNO_2; enhanced degradation of MC-LR was observed with 365 nm UV irradiation, caused by the generation of hydroxyl radicals through the photolysis of HNO_2. The degradation processes of MC-LR could well fit the pseudo-first-order kinetics. Mass spectrometry was applied for identification of the byproducts and the analysis of degradation mechanisms. Major degradation pathways were proposed according to the results of LC–MS analysis. The degradation of MC-LR was initiated via three major pathways: attack of hydroxyl radicals on the conjugated carbon double bonds of Adda, attack of hydroxyl radicals on the benzene ring of Adda, and attack of nitrosonium ion on the benzene ring of Adda.

1. Introduction

Occurrences of water blooms have been reported all around the world. The cyanobacteria species in harmful water bloom such as *Microcystis*, *Oscillatoria*, *Nostoc*, *Aphanizomenon* and *Anabaena*, produce hepatoxin microcystins [1–4]. The senescence and lysis of algae cells release the toxins into water. Over 80 different microcystins have been identified, among which the most common and toxic species found in natural water samples belong to microcystin-LR (MC-LR) [4]. The toxicity of microcystins is exhibited by inhibiting protein phosphatase 1 (PP1) and 2A (PP2A), which lead to liver damage and tumor formation [5]. The degree of damage depends on the amount of toxins and contact time. Longer exposure to microcystins may cause human and livestock deaths [6,7]. Because of its cyclic structure, the degradation process of MC-LR often takes very long time under natural conditions [8]. The threat caused by MCs to human health [9], wildlife [10,11], and ecosystems [12,13] has drawn worldwide attention.

Nitrous acid (HNO_2) and nitrites are prevalent in atmosphere [14] and water bodies, such as rivers, lakes, and oceans [15]; they are usually maintained at low levels. Potential sources for eutrophication including agricultural effluents, industrial discharges, human and livestock wastes, and septic tank effluents would cause the nitrite concentration in water bodies to rise [16,17]. In eutrophic reservoirs, microcystin and nitrite are often detected at the same time [18].

The photolysis of nitrous acid by ultraviolet (UVA) can generate hydroxyl radical (•OH) [19].

$$HNO_2 \xrightarrow{h\nu} {}^{\bullet}OH + NO$$

The hydroxyl radical quantum yield Φ(OH) for the photolysis of nitrous acid at pH 2 was $\Phi = 0.35 \pm 0.02$ over the wavelength range from 280 nm to 385 nm [20]. Hydroxyl radicals are strong oxidants and are able to react with MC-LR on the conjugated double bonds or the benzene ring in the Adda side chain, as well as the double bonds in the cyclic structure. In recent years, catalytic methods and advanced oxidation processes (AOPs) involving hydroxyl radicals such as TiO_2 photolysis method and Fenton method have been widely used for removal of a wide range of pollutants, and they all have been found to be effective in the decomposition of microcystins [21,22]. During the treatment of MC-LR, the diene structure, and the aromatic ring in the Adda side chain are most vulnerable to hydroxyl radical attacking [22–24], from which the degradation of MC-LR is initiated. The MC-LR molecule undergoes degradation through substitution or addition, oxidation, and oxidative bond cleavage.

Nitrosation usually takes place between aromatic compound and nitrous acid through electrophilic substitution of aromatic hydrogen atoms [25]. There have been research studies reporting the photolysis of nitrous acid in the degradation of aromatic

* Corresponding authors. Tel.: +86 21 6564 3343; fax: +86 21 6564 3343.
E-mail addresses: xrxrwang@vip.sina.com (X. Wang), zhqfan@fudan.edu.cn (Z. Fan).

0304-3894/$ – see front matter © 2012 Elsevier B.V. All rights reserved.
doi:10.1016/j.jhazmat.2012.02.033

compounds, during which both nitrosation and hydroxylation were observed [26]. Degradation of MC-LR induced by nitrous acid in the absence of UV was observed in a previous study [27]. In this study, the degradation of MC-LR induced by the photolysis of nitrous acid and degradation mechanisms were investigated for the first time.

2. Materials and methods

2.1. Materials

Microcystin-LR standard was purchased from Express Technology Co., Ltd. (China). HPLC-grade methanol was purchased from Tedia Company (USA). Sodium nitrite ($NaNO_2$), sodium hydroxide (NaOH) and perchloric acid ($HClO_4$) were of analytical grade. C18 cartridges for solid phase extraction of MC-LR were purchased from Supelco Corporation (USA). The 20 W UV lamp (PHILIPS) used for illumination gives off stable irritation of consecutive wavelengths with a maximum intensity at 365 nm.

2.2. Solutions

All the solutions were prepared in deionized water. The concentration of $NaNO_2$ stock solution was 0.10 M and was diluted to a gradient of 0.03 M, 0.015 M, 0.009 M 0.003 M and 0.0015 M for each test. The pH values of the solutions were adjusted by sodium hydroxide solution (NaOH, 0.02 M) or perchloric acid solution ($HClO_4$, 0.2 M, 0.02 M and 0.002 M). MC-LR was extracted and purified from cultured *Microcystis aeruginosa* according to the method previously described [27], and was prepared into stock solutions with concentration gradient (6.52 mg/L, 13.04 mg/L, 19.56 mg/L, and 26.08 mg/L).

2.3. Analytical method

The concentrations of MC-LR in each sample of the kinetic study were determined by a high-performance liquid chromatograph (HPLC, Agilent 1200) equipped with an autosampler (model), an Agilent pump (model), a PDA detector (model) and a ZORBAX SB-C18 column (5 μm, 4.6 mm × 250 mm, Agilent, USA). The mobile phase consisted of 40% acetonitrile and 60% water, both containing 0.05% trifluoroacetic acids (TFA). The flow rate was 1.0 mL/min, and the column temperature was maintained at 40 °C. The injection volume of the sample was 20 μL.

Pseudo-first-order kinetics equation $\ln(c_o/c_t) = kt$ and second-order kinetics equation $1/c_t - 1/c_0 = k_2 t$ were adopted to study the influence of each factors on MC-LR degradation. Theoretical concentrations of HNO_2 were calculated according to the equilibrium of nitrous acid. Variables of MC-LR degradation rate constant k were observed to study the influence of each factor.

Intermediates was analyzed by an LC–MS system, consisted of a Dionex Ultimate 3000 HPLC Pump, a Dionex Ultimate 3000 autosampler and a Bruker micrOTOFIIMass Spectrometer with electrospray ionization source. The HPLC column was ZORBAX SB-C18 column (5 μm, 4.6 mm × 250 mm, Agilent, USA). Mobile phase was water and acetonitrile, both containing 0.05% acetic acid. Gradient elution method was programmed according to Liu et al. [23]. The column temperature was maintained at 40 °C and the flow rate was controlled at 1.0 mL/min. The injection volume of the treated sample was 80 μL. The mass spectra data were obtained in the positive ion mode by full scanning from m/z 400 to 1200.

Analysis of breakdown products of MC-LR in the reaction process of combination of UV and nitrous acid was based on the mass spectrum in the LC–MS chromatogram. Major byproducts were identified according to molecular weight and corresponding peak time. Reaction pathways were proposed according to the results of LC–MS analysis.

2.4. Experimental procedure

Experiments were carried out to investigate the effect of different factors including $NaNO_2$ concentrations (actually existed in the ionization equilibrium of NO_2^- and HNO_2 under different pH values), pH values, MC-LR concentration and UV intensity. Duplicate experiments were conducted.

In this study, the volume of the reaction solutions was divided into quotas for each stock solution, with 1.0 mL for $NaNO_2$ stock solution, 0.5 mL for $HClO_4$ or NaOH stock solution, and 1.5 mL for MC-LR stock solution. All the stock solutions were mixed as the reaction solution. Variants of each factor were adjusted by the same volume of stock solutions of each concentration gradient. The pH value was determined with a pH meter (FE20, Mettler-Toledo Instruments Co., Ltd.) before the reaction solution was transferred into the quartz reactor. The reactor was sealed with a PTFE cap and septum, and 150 μL of samples were obtained with an injector during the whole degradation process. Before HPLC analysis, the acidic and alkaline samples were neutralized with 50 μL NaOH or $HClO_4$ solutions of three times the concentration in the reaction solution, and 50 μL water was added in the samples without NaOH or $HClO_4$. The temperature was maintained at 25 ± 1 °C. Reaction solution containing 5.0 mM nitrite ion ($HNO_2 + NO_2^-$) and 100 mg/L MC-LR standard (pH 1.60) was exposed to 3000 μW/cm^2 UV irradiation for LC–MS analysis.

3. Results and discussion

3.1. MC-LR degradation under different experimental conditions

The degradation was influenced by major initial conditions including pH value, $NaNO_2$ concentration, MC-LR concentration, and UV intensity. Preferable degradation of MC-LR was observed under acid conditions in the presence of sodium nitrite and UV irradiation. To study the effect of each factor, a preferable reaction time of 1 h was adopted. Under favorable condition of pH 1.61, 5.0 mM $NaNO_2$, 9.78 mg/L MC-LR, and 3000 μW/cm^2 UV irradiation, the MC-LR degradation rate could reach 97.6% at t = 1 h. Experiments were carried out to evaluate the influence of each factor.

3.2. Effect of pH value on MC-LR degradation

With the same $NaNO_2$ concentrations and MC-LR concentrations in the reaction solutions and UV intensity, MC-LR degradation rate increased when the pH value was lowered. Under each pH values (pH 1.61, pH 3.12, pH 4.50, pH 6.88, and pH 9.88) in this study, the maximum MC-LR degradation rate occurred at pH 1.61 (Fig. 1), with the pseudo-first-order kinetic constant k of 6.49×10^{-2} min^{-1} and MC-LR removal rate of 97.6%. The k values decreased with the pH value increased. When the pH value of the reaction solution increased to 9.88, the pseudo-first-order kinetic constant k dropped to 1.19×10^{-3} min^{-1} and MC-LR removal rate was 7.40%. Acidic condition could promote the rate of MC-LR degradation in this study.

3.3. Effect of $NaNO_2$ concentration

The $NaNO_2$ concentration also played an indispensable role in the degradation of MC-LR. The $NaNO_2$ concentrations observed in this study ranged from 0 mM to 10.0 mM. Under acid conditions (adjusted by the same amount of perchloric acid) with the same MC-LR concentration and UV intensity, The pseudo-first-order kinetic constant k increased from 1.32×10^{-2} min^{-1} to 9.62×10^{-2} min^{-1}, and the MC-LR removal rate increased from 53.2% to 99.2% when the $NaNO_2$ concentration increased from 0.5 mM to 10.0 mM respectively. In the absence of $NaNO_2$

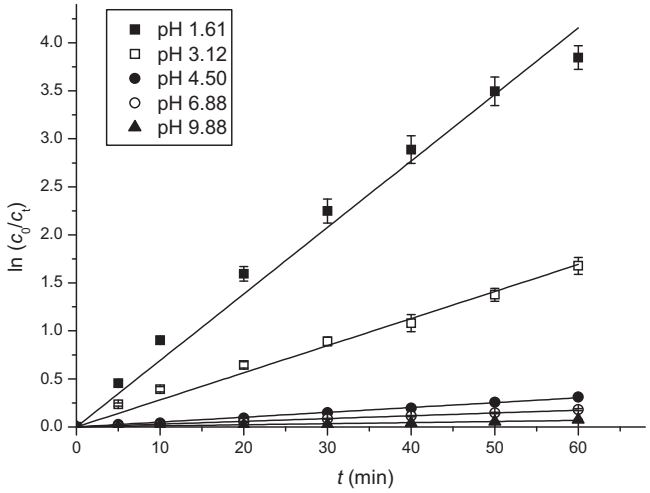

Fig. 1. Pseudo-first-order kinetics of MC-LR degradation under different pH values. Equation $\ln(c_o/c_t) = kt$ was adopted to describe the degradation processes, and the slope k is the pseudo-first-order kinetic constant. The reaction solutions contains 5.0 mM $NaNO_2$, 9.78 mg/L MC-LR. 3000 μW/cm² UV irradiation at 25 ± 1 °C.

(0 mM), the pseudo-first-order kinetic constant k value was 3.45×10^{-4} min^{-1}, which was negligible comparing to the major degradation processes (Fig. 2). This could exclude the possibility that the MC-LR was degraded by perchloric acid and demonstrated that the UV alone had little effect on the degradation of MC-LR. Under the same $NaNO_2$ concentration, MC-LR degradation rate decreased as the pH value increased, so the primary condition for MC-LR degradation is the presence of nitrous acid, which was observed in the previous study [25].

The nitrite ion (NO_2^-) was provided by $NaNO_2$ and exists in ionization equilibrium with HNO_2:

$$HNO_2 \rightarrow H^+ + NO_2^- \quad pK_a = 3.3$$

According to the pH value and the concentration of $NaNO_2$, the theoretical concentration of HNO_2 can be calculated (Table 1).

Contrary to the results in the previous study that the pseudo-first-order kinetic constant k reached the maximum at the $NaNO_2$ concentration of 5.0 mM in the absence of UV, the pseudo-first-order kinetic constant k keeps increasing when the $NaNO_2$ concentration increased from 0 mM to 10.0 mM in the presence of UV irradiation. The increase in $NaNO_2$ concentration ensured the more HNO_2 available for photolysis to generate hydroxyl radicals, thus could enhance the degradation of MC-LR caused by hydroxyl radical oxidation.

Table 1
Theoretical concentration of HNO_2 in the reaction solutions.

$c(NaNO_2)$ (mM)	pH	$c(HNO_2)$ (mM)	% [HNO_2/($HNO_2 + NO_2^-$)]
0.50	1.51	0.49	98.4
1.00	1.52	0.98	98.2
3.00	1.56	0.30	98.0
5.00	1.61	4.90	98.0
10.0	1.62	9.80	98.0

3.4. Effect of UV intensity

Five levels of UV intensities (0 μW/cm², 958 μW/cm², 1972 μW/cm², 3000 μW/cm², and 4250 μW/cm²) were adopted in illumination in the process of MC-LR degradation. When the UV increased from 0 μW/cm² to 4250 μW/cm², the degradation kinetic constant k increased from 1.42×10^{-2} min^{-1} to 8.15×10^{-2} min^{-1} (Fig. 3), and MC-LR removal rate increased from 60.1% to 98.9%. Since the photo degradation of MC-LR does not occur under visible or UVA radiation [28], the results suggest there is a synergistic effect between UV and nitrous acid on MC-LR degradation.

The enhancement of removal efficiency was probably caused by the increased concentration of hydroxyl radical generated from the photolysis of nitrous acid. With the same quantum yield of hydroxyl radical, the increase of UV intensity could lead more hydroxyl radicals generated within the same time period, directly resulting in the higher removal rate of MC-LR. UV intensity was an important factor influencing the efficiency of degradation.

3.5. Effect of MC-LR concentration

The degradation process of MC-LR is also influenced by its concentrations. As the MC-LR concentrations increased from 3.26 mg/L to 13.04 mg/L, the pseudo-first-order kinetic constant k decreased from 0.116 min^{-1} to 0.051 min^{-1} (Fig. 4), and the removal rate of

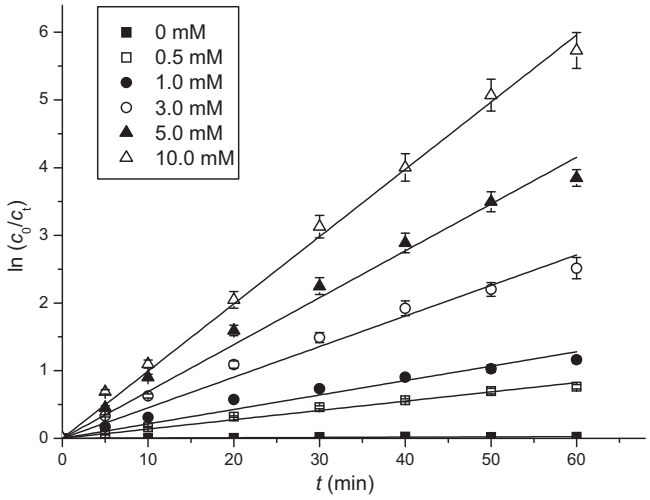

Fig. 2. Pseudo-first-order kinetics of MC-LR degradation under different $NaNO_2$ concentrations. Equation $\ln(c_o/c_t) = kt$ was adopted to describe the degradation processes. Reaction solutions contains 0.5 mL $HClO_4$ stock solution, 9.78 mg/L MC-LR. 3000 μW/cm² UV irradiation at 25 ± 1 °C.

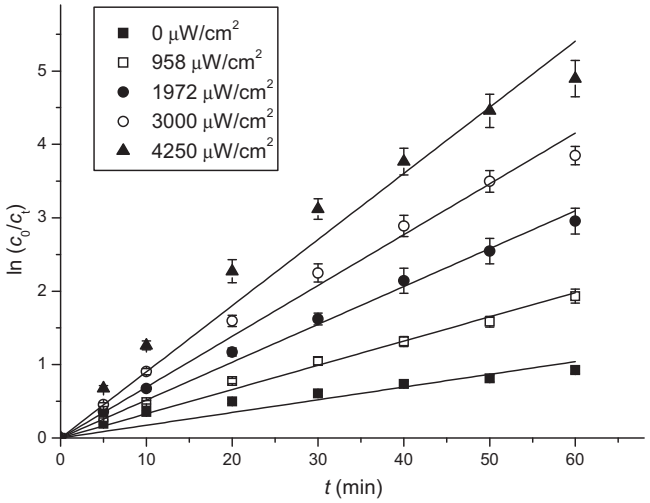

Fig. 3. Pseudo-first-order kinetics of MC-LR degradation under different UV intensities. Equation $\ln(c_o/c_t) = kt$ was adopted to describe the degradation processes. The reaction solutions contains 0.5 mL $HClO_4$ stock solution, 5.0 mM $NaNO_2$, 9.78 mg/L MC-LR, 25 ± 1 °C.

MC-LR dropped from 98.9% to 95.0%, but the initial MC-LR degradation rate increased from 0.270 mg/L min^{-1} to 0.473 mg/L min^{-1}. The yield rate of hydroxyl radical remains constant with the same HNO_2 concentration and UV intensity. Although the absolute degradation rate increased, the increasing MC-LR concentration resulted in a decreased in the ratio of amount of MC-LR decomposed in the total amount of MC-LR.

All the degradation processes discussed above could be described by pseudo-first-order kinetics and second-order kinetics, and the factors are listed in Table 2.

3.6. MC-LR degradation mechanisms

More than 10 intermediates were identified from the LC–MS spectrogram. According to their *m*/*z* value, peak time and abundance in each sample, they could be identified as intermediates or final products. Ions with *m*/*z* values greater than 995.5 (MC-LR) appeared in the beginning of UV irradiation and disappeared gradually. These ions were usually identified as initial intermediates, with added group on the MC-LR molecule. Ions with smaller *m*/*z* values were seen as break down intermediates or final products.

According to the degradation mechanisms with hydroxyl radicals described in previous studies [22–24] and the reaction between nitrous acid and MC-LR under UV irradiation, the breakdown of MC-LR molecule was initiated by addition of hydroxyl radicals or substitution of nitrosonium ions. Major target sites are the double bonds in the Adda moiety or the cyclic structure of the MC-LR structure for hydroxyl radicals, and the benzene ring at the end of the Adda moiety for nitrosonium ions. Major degradation pathways in this study were proposed as follows.

3.6.1. Attack of hydroxyl radicals on the conjugated carbon double bonds of Adda

Attack of hydroxyl radicals on the conjugated carbon double bonds of Adda moiety of MC-LR molecule has been proved to be the major degradation pathway of MC-LR [29]. There have been many research studies reporting the hydroxyl radicals addition on the conjugated dienes of the MC-LR molecule, which occurs through the process of 1, 2 additions, or 1, 4 additions [24]. The adducts then undergo through further degradation processes and form intermediates of smaller molecular weights. This degradation pathway have been characterized with the detection of the byproducts with *m*/*z* of 1029.5 in the LC–MS chromatogram, which corresponds to two hydroxyl radicals added onto the conjugated structure to form the dihydroxy-MC-LR intermediates (product 1a, 1b, and 1c). Cleavage products with $(M+H)^+$ ions at *m*/*z* 795.4 and *m*/*z* 835.4 were detected, which indicated that the intermediate then went through cleavage of the Adda side chain.

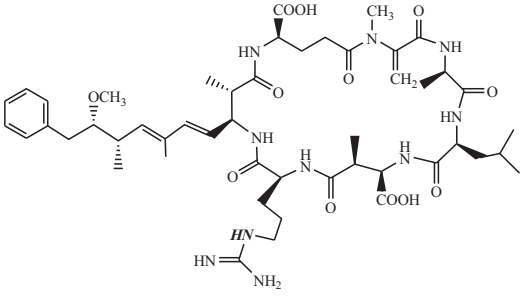

MC-LR ($C_{49}H_{74}N_{10}O_{12}$)
Mass: 994.5
m/z: 995.5

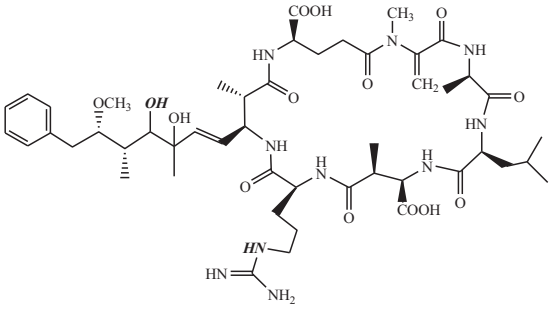

product 1a ($C_{49}H_{76}N_{10}O_{14}$)
Mass: 1028.5
m/z: 1029.5

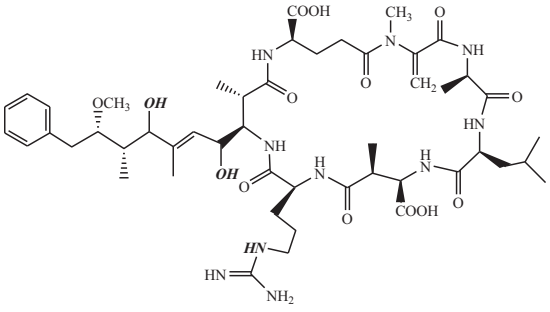

product 1b ($C_{49}H_{76}N_{10}O_{14}$)
Mass: 1028.5
m/z: 1029.5

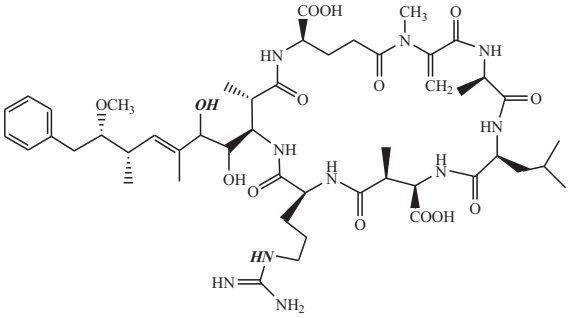

product 1c ($C_{49}H_{76}N_{10}O_{14}$)
Mass: 1028.5
m/z: 1029.5

Further breakdown processes of MC-LR and adducts occur through destruction of the cyclic structure of the MC-LR molecule caused by hydroxyl radicals. Intermediates can be oxidized into corresponding carboxylic acids [23]. Product *m*/*z* 811.3 detected can be seen as evidence of this degradation pathway.

The conjugated double bonds in the Adda side chain are responsible for the PP1 and PP2A inhibition [30–32], and the conjugated double bonds in the Adda moiety can cause a characteristic absorption maximum at 238 nm [33]. In the treatment of UV and nitrous acid, the absorption intensity of MC-LR was weakened with time, which indicated that the Adda moiety have been destroyed during the treatment. Intermediates without the conjugated double bonds have been reported to be less toxic. Reaction between hydroxyl radicals and microcystin-LR has been proved to be an effective treatment method in detoxification of microcystin-LR [34].

Table 2
Kinetics of MC-LR degradations in different reactions.

Conditions				Pseudo-first-order kinetics $\ln(c_0/c_t) = k_1 t$		Second-order kinetics $1/c_t - 1/c_0 = k_2 t$	
pH	$NaNO_2$ (mM)	MC-LR (mg/L)	UV ($\mu W/cm^2$)	k_1 (min^{-1})	R^2	k_2 ($g^{-1}\,L\,min^{-1}$)	R^2
1.61	5.0	9.78	3000	0.0649	0.98871	0.106	0.88843
3.12	5.0	9.78	3000	0.0263	0.99261	0.00925	0.93988
4.50	5.0	9.78	3000	0.00521	0.99693	7.40×10^{-4}	0.99119
6.88	5.0	9.78	3000	0.00304	0.99688	3.90×10^{-4}	0.99371
9.88	5.0	9.78	3000	0.00119	0.95927	1.44×10^{-4}	0.93988
1.51	0	9.78	3000	3.45×10^{-4}	0.66141	5.00×10^{-5}	0.95494
1.51	0.5	9.78	3000	0.0132	0.9847	0.003	0.9969
1.52	1.0	9.78	3000	0.0190	0.97002	0.00555	0.99934
1.56	3.0	9.78	3000	0.0415	0.98489	0.0304	0.95507
1.62	10.0	9.78	3000	0.0962	0.99694	0.383	0.84613
1.58	5.0	3.26	3000	0.116	0.97694	0.829	0.97664
1.60	5.0	6.52	3000	0.0829	0.98614	0.345	0.89214
1.62	5.0	13.04	3000	0.0507	0.98553	0.0387	0.93017
1.61	5.0	9.78	0	0.0142	0.93671	0.00385	0.98498
1.61	5.0	9.78	958	0.0303	0.99112	0.0139	0.93781
1.61	5.0	9.78	1972	0.0486	0.99418	0.0426	0.90326
1.61	5.0	9.78	4250	0.0815	0.97581	0.0319	0.8899

As the photolysis process continued, the initially increasing abundance of the intermediates to intensity around 10,000 subsequently decreased to below 1000. In the mass spectrum at 60 min, the peaks of the intermediates could hardly be discerned from the signal noises, which could be interpreted that total mineralization had occurred intermediates had been further oxidized to final products [23,24].

3.6.2. Attack of hydroxyl radicals on the benzene ring of Adda

The hydroxyl radicals are highly reactive and can go through substitution reaction against the hydrogen atom on the benzene ring to form the hydroxylated MC-LR adducts [35]. The second order kinetic constant of the reaction of hydroxyl radicals with the aromatic ring is slightly higher compared to alkenes [36]. So the intermediate m/z 1011.5 (product 2) was reached a detectable abundance at 2 min, prior to the detection of intermediated m/z 1029.5 at 5 min. Intermediate m/z 1011.5 corresponds to the product with the hydrogen atom in the aromatic ring substituted by a hydroxyl group, and the Adda side chain acts as a guide for para or ortho substitution of aromatic hydrogen atoms.

Under acidic condition, phenols are easy to form the aromatic cations [37]. Accordingly, the hydroxylated MC-LR adduct (product 2) reacts with H^+ to form the MC-LR^+ ion (product 2a) through the following reaction:

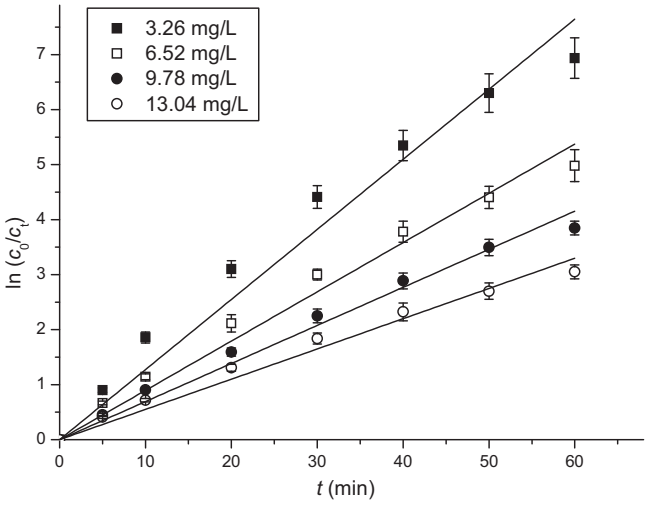

Fig. 4. Pseudo-first-order kinetics of MC-LR degradation under different MC-LR concentrations. Equation $\ln(c_o/c_t) = kt$ was adopted to describe the degradation processes. The reaction solutions contains 0.5 mL $HClO_4$ stock solution, 5.0 mM $NaNO_2$. 3000 $\mu W/cm^2$ UV irradiation at 25 ± 1 °C.

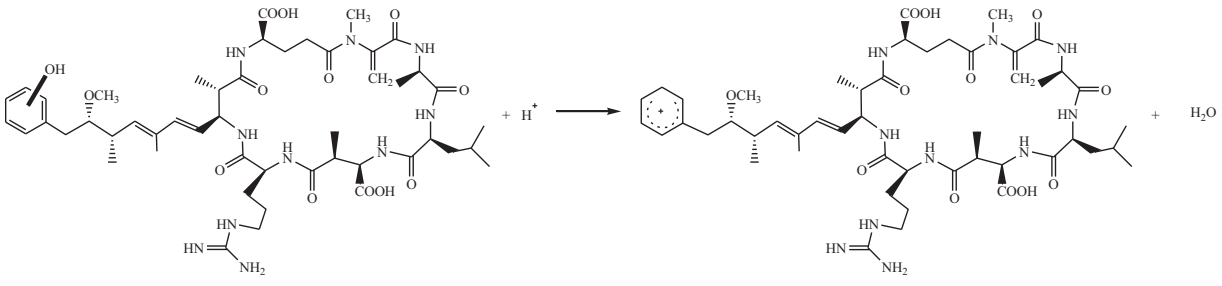

product 2 ($C_{49}H_{74}N_{10}O_{13}$)
Mass: 1010.5
m/z: 1011.5

product 2a ($C_{49}H_{73}N_{10}O_{12}$)
Mass: 993.5
m/z: 497.3

The adducts hydroxylated MC-LR (product 2) and MC-LR$^+$ ion (product 2a) correspond to the intermediates $(M+H)^+$ m/z 1011.5 and $(M+H)^{2+}$ m/z 497.3 in the LC–MS analysis. This can be seen as evidence to this proposed reaction pathway.

3.6.3. Attack of nitrosonium ion on the benzene ring of Adda

Under acidic conditions nitrous acid is protonized to form the nitrous acidium ion $H_2NO_2^+$ and the nitrosonium ion NO^+ through the following reactions [38,39]:

$$H^+ + HNO_2 \overset{K}{\rightleftharpoons} H_2NO_2^+$$

$$H_2NO_2^+ \underset{k_{-2}}{\overset{k_2}{\rightleftharpoons}} NO^+ + H_2O$$

The nitrosonium ion (NO^+) is a strong electrophilic reagent, which is easy to react with aromatic compounds. The benzene ring at the end of the Adda group of the MC-LR molecule is vulnerable to nitrosonium ion and is easy to form the corresponding intermediates in the process of nitrosation. Possible reaction pathways are proposed as follows:

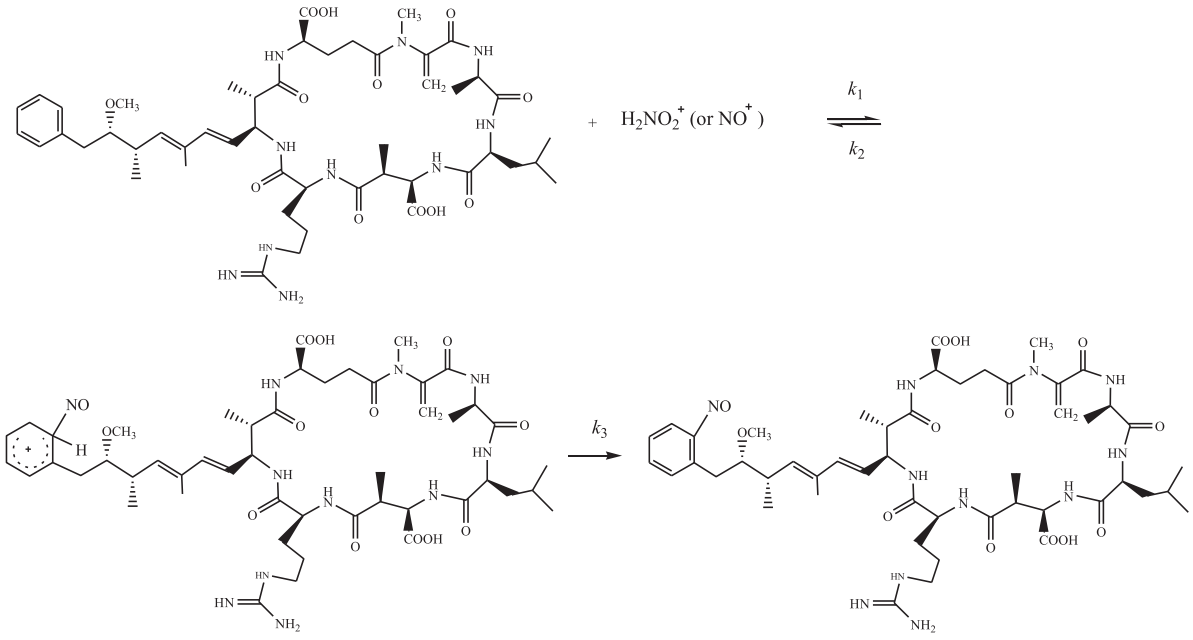

product 3a ($C_{49}H_{74}N_{11}O_{13}$)
Mass: 1024.5
m/z: 512.8

product 3 ($C_{49}H_{73}N_{11}O_{13}$)
Mass: 1023.5
m/z: 1024.5

This reaction pathway is evidenced by the detection of intermediates *m*/*z* 1024.5 (product 3) and product *m*/*z* 512.8 (product 3a) in mass spectrogram.

Under UV irradiation, nitrosation may occur at the same time with hydroxylation, and the MC-LR hydroxylated adduct may also go through nitrosation process:

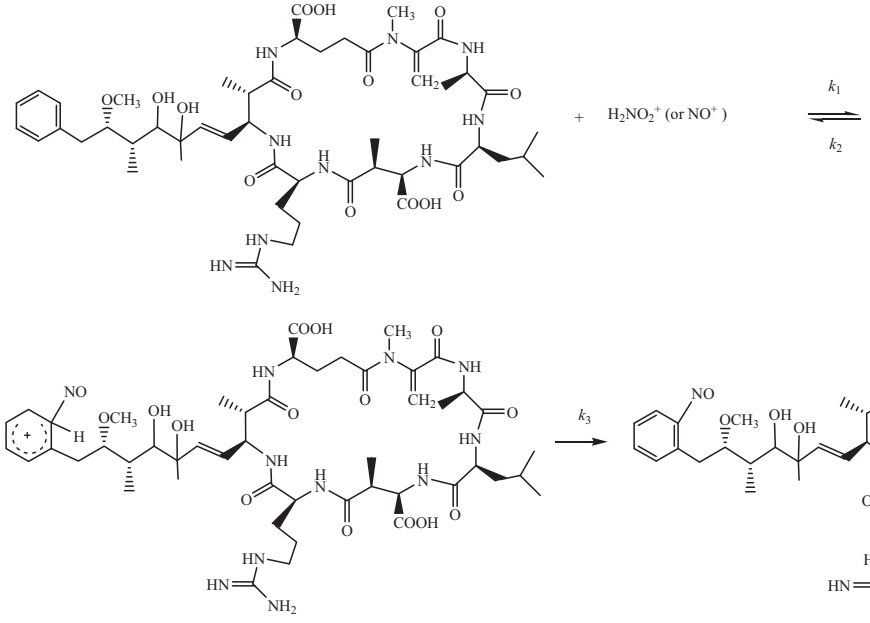

product 4a ($C_{49}H_{76}N_{11}O_{15}$)
Mass: 1058.5
m/z: 529.8

product 4 ($C_{49}H_{75}N_{11}O_{15}$)
Mass: 1057.5
m/z: 1058.5

Intermediates with *m*/*z* 1058.5 and *m*/*z* 529.8 were the adducts of two hydroxyl radicals, either on the conjugated double bonds of the Adda side chain or on the cyclic structure of the MC-LR molecule. Further analysis is required to determine the site of the hydroxylation occurs.

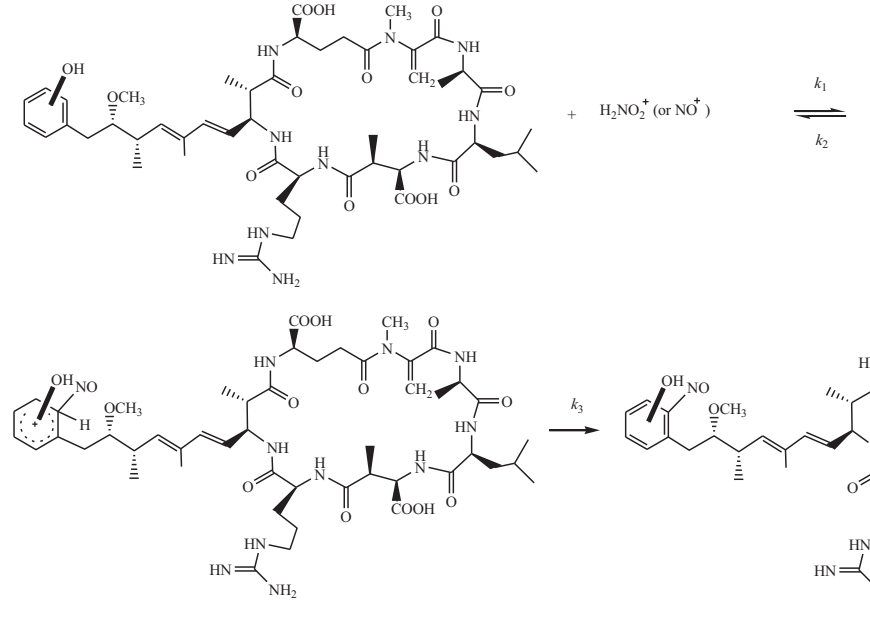

product 5a ($C_{49}H_{74}N_{11}O_{14}$)
Mass: 1040.5
m/z: 520.8

product 5 ($C_{49}H_{73}N_{11}O_{14}$)
Mass: 1039.5
m/z: 1040.5

Other intermediates detected included product *m*/*z* 1040.5 and product *m*/*z* 520.8. Intermediate *m*/*z* 1040.5 (product 5) was the adduct of hydroxyl on the benzene ring of Adda side chain, which coexisted with product *m*/*z* 520.8 (product 5a).

4. Conclusions

The degradation of MC-LR in solutions by nitrous acid under UV irradiation was investigated in this research. The degradation rate of MC-LR was influenced by factors including pH value, sodium nitrite concentration, MC-LR concentration and UV intensity. Pseudo-first-order kinetics and second-order kinetics were adopted to describe the degradation process.

The necessary condition of MC-LR degradation was the presence of nitrite under acidic condition, so the degradation was caused by HNO_2, which was co-determined by the initial $NaNO_2$ concentration and the initial pH value. Enhanced degradation rate was observed in the presence of UV irradiation. The pseudo-first-order kinetic constant k increased with the increase of $NaNO_2$ concentration and UV intensity, and decrease with the increase of pH value and MC-LR concentration.

Major intermediates in the degradation process of MC-LR were identified, and the degradation mechanisms could be proposed as the following major pathways: 1. Attack of hydroxyl radicals on the conjugated carbon double bonds of Adda; 2. Attack of hydroxyl radicals on the benzene ring of Adda; 3. Attack of nitrosonium ion on the benzene ring of Adda.

The toxicity of inhibition of PP1 and PP2A was expected to be eliminated as a result of the destruction of the conjugated double bonds in the Adda side chain by hydroxyl radicals generated during the photolysis of nitrous acid. Intermediates could be further decomposed to final products.

It is reasonable that the cyanotoxins with the Adda moiety and the double bonds structure may also go through the same modification and degradation process in the treatment of UV and nitrous acid. In the existence of nitrous acid/nitrite, intense ultraviolet in the sunlight can be a best catalyst for the degradation of cyanotoxins. The results of this research provide a new approach for the study of cyanotoxins degradation in engineering application and in the natural environment.

Because of the nitrosation process occurred in the degradation of MC-LR, specific investigation of the complete degradation process, and the properties of the reaction intermediates and products formed during the treatment of UV and nitrous acid/nitrite, require further study.

Acknowledgment

This work was supported by the Key Laboratory Open Fund of Fishery Ecology Environment, Ministry of Agriculture, China.

References

[1] G.A. Codd, Cyanobacterial toxins: occurrence, properties and biological significance, Water Sci. Technol. 32 (1995) 149–156.
[2] K. Harada, Recent advances of toxic cyanobacteria researches, J. Health Sci. 45 (1999) 150–165.
[3] M.E. van Apeldoorn, H.P. van Egmond, G.J. Speijers, G.J. Bakker, Toxins of cyanobacteria, Mol. Nutr. Food Res. 51 (2007) 7–60.
[4] I. Chorus, Cyanotoxins: Occurrence Causes and Consequences, Springer, Berlin, 2001.
[5] R. Nishiwaki-Matsushima, T. Ohta, S. Nishiwaki, M. Suganuma, K. Kohyama, T. Ishikawa, W.W. Carmichael, H. Fujiki, Liver tumor promotion by the cyanobacterial cyclic peptide toxin microcystin-LR, J. Cancer Res. Clin. 118 (1992) 420–424.
[6] P.R. Hawkins, M.T.C. Runnegar, A.R.B. Jackson, I.R. Falconer, Severe hepatotoxicity caused by the tropical cyanobacterium (blue-green alga) *Cylindrospermopsis raciborskii* (Wolozynska) Seenaya and Subba Raju isolated from a domestic water supply reservoir, Appl. Environ. Microbiol. 50 (1985) 1292–1295.
[7] W.W. Carmichael, S. Azevedo, J.S. An, R.J. Molica, E.M. Jochimsen, Human fatalities from cyanobacteria: chemical and biological evidence for cyanotoxins, Environ. Health Perspect. 109 (2001) 663–668.
[8] K. Harada, K. Tsuji, Persistence and decomposition of hepatotoxic microcystins produced by cyanobacteria in natural environment, J. Toxicol. Toxin Rev. 17 (1998) 385–403.
[9] S.M.F.O. Azevedo, W.W. Carmichael, E.M. Jochimsen, K.L. Rinehardt, S. Lau, G.R. Shaw, G.K. Eaglesham, Human intoxication by microcystins during renal dialysis treatment in Caruaru, Brazil, Toxicology 181–182 (2002) 441–446.
[10] A.P. Negri, G.J. Jones, M. Hindmarsh, Sheep mortality associated with paralytic shellfish poisons from the cyanobacterium *Anabaena circinalis*, Toxicon 33 (1995) 1321–1329.
[11] J.F. Briand, S. Jacquet, C. Bernard, J.F. Humbert, Health hazards for terrestrial vertebrates from toxic cyanobacteria in surface water ecosystems, Vet. Res. 34 (2003) 361–377.
[12] G. Francis, Poisonous Australian lake, Nature 18 (1978) 11–12.
[13] J.H. Landsberg, The effects of harmful algal blooms on aquatic organisms, Rev. Fish. Sci. 10 (2002) 113–390.
[14] A.R. Reisinger, Observations of HNO_2 in the polluted winter atmosphere: possible heterogeneous production on aerosols, Atmos. Environ. 34 (2000) 3865–3874.
[15] P.N. Okafor, U.I. Ogbonna, Nitrate and nitrite contamination of water sources and fruit juices marketed in South-Eastern Nigeria, J. Food Compos. Anal. 16 (2003) 213–218.
[16] T. Jones, Poison: nitrate/nitrite, In Practice 15 (1993) 146–147.
[17] V.A. Razumov, F.I. Tyutyunova, Nitrite contamination of the Moskva River: causes and effects, Water Resour. 28 (2001) 324–334.
[18] W.T. Brant, M.B. Joann, H.A. Elie, Eutrophication and cyanobacteria blooms in run-of-river Impoundments in North Carolina, USA, Lake Reserv. Manage. 23 (2007) 179–192.
[19] B. Alicke, A. Geyer, A. Hofzumahaus, F. Holland, S. Konrad, H.W. Patz, J. Schafer, J. Stutz, A. Volz-Thomas, U. Platt, OH formation by HONO photolysis during the BERLIOZ experiment, J. Geophys. Res. 108 (2003) 8247, doi:10.1029/2001JD000579.
[20] M. Fischer, P. Warneck, Photodecomposition of nitrite and undissociated nitrous acid in aqueous solution, J. Phys. Chem. 100 (1996) 18749–18756.
[21] E.R. Bandala, D. Martínez, E. Martínez, D.D. Dionysiou, Degradation of microcystin-LR toxin by Fenton and Photo-Fenton processes, Toxicon 43 (2004) 829–832.
[22] I. Liu, L.A. Lawton, B. Cornish, P.K.J. Robertson, Mechanistic and toxicity studies of the photocatalytic oxidation of microcystin-LR, J. Photochem. Photobiol. A 148 (2002) 349–354.
[23] I. Liu, L.A. Lawton, P.K.J. Robertson, Mechanistic studies of the photocatalytic oxidation of microcystin-LR: an investigation of byproducts of the decomposition process, Environ. Sci. Technol. 37 (2003) 3214–3219.
[24] M.G. Antoniou, J.A. Shoemaker, A.A. Delaceuz, D.D. Dionysiou, Unveiling new degradation intermediates/pathways from the photocatalytic degradation of microcystin-LR, Environ. Sci. Technol. 42 (2008) 8877–8883.
[25] S. Gonzaĭlez-Mancebo, M.P. Garcıĭa-Santos, J. Hernaĭndez-Benito, E. Calle, J. Casado, Nitrosation of phenolic compounds: inhibition and enhancement, J. Agric. Food Chem. 47 (1999) 2235–2240.
[26] D. Vione, V. Maurino, C. Minero, M. Lucchiari, E. Pelizzetti, Nitration and hydroxylation of benzene in the presence of nitrite/nitrous acid in aqueous solution, Chemosphere 56 (2004) 1049–1059.
[27] Q.W. Ma, J. Ren, H.H. Huang, X.R. Wang, S.B. Wang, Q. Luo, Z.Q. Fan, A novel degradation method of microcystin-LR induced by nitrous acid, Fresenius Environ. Bull. 20 (2011) 1007–1012.
[28] W. Song, S. Bardowell, K.E. O'Shea, Mechanistic study and the influence of oxygen on the photosensitized transformations of microcystins (cyanotoxins), Environ. Sci. Technol. 41 (2007) 5336–5341.
[29] L.A. Lawton, P.K.J. Robertson, B.J.P.A. Cornish, M. Jaspars, Detoxification of microcystins(cyanobacterial hepatotoxins) using TiO_2 photocatalytic oxidation, Environ. Sci. Technol. 33 (1999) 771–775.
[30] B.M. Gulledge, J.B. Aggen, H.B. Huang, A.C. Nairn, A.R. Chamberlin, The microcystins and nodularins: cyclic polypeptide inhibitors of PP1 and PP2A, Curr. Med. Chem. 9 (2002) 1991–2003.
[31] B.M. Gulledge, J.B. Aggen, H. Eng, K. Sweimeh, A.R. Chamberlin, Microcystin analogues comprised only of Adda and a single additional amino acid retain moderate activity as PP1/PP2A inhibitors, Bioorg. Med. Chem. Lett. 13 (2003) 2907–2911.
[32] J. Goldberg, H.B. Huang, Y.G. Kwon, P. Greengard, A.C. Nairn, J. Kuriyan, Three-dimensional structure of the catalytic subunit of protein serine/threonine phosphatase-1, Nature 376 (1995) 2100–2105.
[33] J. McElhiney, L.A. Lawton, Detection of the cyanobacterial hepatotoxins microcystins, Toxicol. Appl. Pharmacol. 203 (2005) 219–230.
[34] C. Svrcek, D.W. Smith, Cyanobacteria toxins and the current state of knowledge on water treatment options: a review, J. Environ. Eng. Sci. 3 (2004) 155–185.
[35] L. Cermenati, P. Pichat, C. Guillard, A. Albini, Probing the TiO_2 photocatalytic mechanisms in water purification by use of quinoline, photo-fenton generated OH radicals and superoxide dismutase, J. Phys. Chem. B 101 (1997) 2650–2658.
[36] G.V. Buxton, C.L. Greenstock, W.P. Helman, A.B. Ross, Critical review of rate constants for reactions of hydratedelectrons, hydrogen atoms and hydroxyl radicals ($^{\bullet}OH/^{\bullet}O^{-}$) inaqueous solution, J. Phys. Chem. Ref. Data 17 (1988) 513–886.
[37] K. Sehested, E.J. Hart, Formation and decay of the biphenyl cation radical in aqueous acidic solution, J. Phys. Chem. 79 (1975) 1639–1642.
[38] S. Abhijit, G. Sara, C. Diane, C. Gidon, Determination of optimal conditions for synthesis of peroxynitrite by mixing acidified hydrogen peroxide with nitrite, Free Radical Biol. Med. 24 (1998) 653–659.
[39] N.S. Bayliss, R. Dingle, D.W. Watts, R.J. Wilkie, The spectrophotometry of sodium nitrite solutions in aqueous sulphuric and perchloric acids and the equilibrium between nitrosonium ion and nitrous acid, Aust. J. Chem. 16 (1963) 933–942.